Electrical and Mechanical Properties of Expanded Graphite-Reinforced High-Density Polyethylene

Wenge Zheng,[1] Xuehong Lu,[1] Shing-Chung Wong[2]

[1]*School of Materials Engineering, Nanyang Technological University, Nanyang Avenue, 639798, Singapore*
[2]*Department of Mechanical Engineering and Applied Mechanics, North Dakota State University, Fargo, North Dakota 58105*

Received 21 April 2003; accepted 22 July 2003

ABSTRACT: High-density polyethylene (HDPE) was reinforced with expanded and untreated graphite in a melt-compounding process. Viscosity increased upon addition of graphite phase, with the expanded graphite (EG) showing more dramatic rise than the untreated graphite (UG) in viscosity. The increase in viscosity was attributed to the increased surface-to-volume ratio for the EG filler after acid treatment. Electrical conductivity also increased from that pertaining to an insulator to one characteristic of a semiconductor. The EG system showed a lower percolation threshold for transition in conductivity compared to that in the UG system. DSC results indicated that the fillers acted as a nucleating agent in inducing the crystallization of HDPE in the composites. However, the overall degree of crystallinity and melting temperature of HDPE decreased with the addition of EG and UG. Mechanical properties improved as a function of filler content but the overall enhancement was not impressive. It was conjectured that the filler–matrix interface was not optimized in the melt-mixing process. However, the role of EG as a reinforcement phase for both electrical and mechanical properties was unambiguously established. The EG composites demonstrated potentially useful attributes for antistatic, barrier, mechanical, electrical, and cost-effective applications. © 2004 Wiley Periodicals, Inc. J Appl Polym Sci 91: 2781–2788, 2004

Key words: expanded graphite; nanocomposites; conductivity; reinforcement; mechanical properties

INTRODUCTION

Nanocomposites have been actively studied in light of the potential benefits derived from nanoscale phenomena and engineering. The two nanoscale composite systems that spurred a flurry of investigations since the early 1990s are organo-modified clay-reinforced polymers[1–3] and carbon nanotubes.[4–6] What has received little attention is the graphene-based nanocomposite system that can provide cost-effective processing and excellent functional properties. The attempt to process nanoclay-reinforced polymers in mass production quantities has been fraught with difficulties in exfoliating the clay particles in nonpolar polymer matrices such as polypropylene[7–9] and epoxies.[10,11] Most organoclay systems reported thus far are intercalated rather than truly exfoliated. For those that were able to display uniformly dispersed clay particles, the benefits were limited to mechanical and barrier improvements.[12–14] Alternatively, the development of carbon nanotubes (CNT) appeared to accomplish what nanoclay could not have achieved. CNT-reinforced polymers[15–17] were able to provide a wider array of functional properties compared to clay-reinforced systems. However, processing of CNT is presently prohibitively expensive for mass production.

Graphene-based nanocomposites possess potential applications in radiation and electromagnetic shielding, antistatic, shrinkage- and corrosion-resistant coatings, and other mechanical and functional attributes such as stiffness, barrier, and conducting capabilities.[18–24] Most engineering polymers are inherent insulators, which have traditionally produced excellent substrates in electronic packages and lightweight applications. They can become conducting when doped with conducting particles, such as carbon black (CB),[18,19] metallic powder,[20–22] polyaniline,[23] and graphite.[24] Improvement in electrical conductivity arising from the increase of filler content was observed for most conductive composites containing CB and metal powder.[18–22] The electrical resistivity of such a composite is well explained by the percolation theory.[25–28] With a small volume fraction of the conducting filler particles, the resistivity of the composite is close to that of an insulating polymer. As the volume fraction of the filler increases, the particles form a conductive network in the composite. As a result, the electrical conductivity increases by several orders of magnitude at the percolation threshold.

Correspondence to: S.-C. Wong (Josh.Wong@ndsu.nodak.edu).

Contract grant sponsor: Nanyang Technological University; contract grant number: RGM–47/00.

Contract grant sponsor: ND NASA EPSCoR; contract grant number: NASA NCC5-582.

Journal of Applied Polymer Science, Vol. 91, 2781–2788 (2004)

What we attempted in this study was to investigate a mass production method for graphene-based nanocomposites. Earlier[29,30] we examined an acid treatment that could considerably expand the graphite sublayers, allowing the percolation threshold for electrical conductivity to drop to less than 1 wt %. This technique does not require a costly purification process[31] but could emulate the efficiency of CNT-reinforced polymers when simple mechanical attrition techniques were introduced. Natural flake graphite possesses good in-plane electrical conductivity of 10^4 S/cm at ambient temperature.[32] They could be intercalated by modification with various chemical species to form the graphite intercalation compounds (GIC).[29,30,33–37] Subjecting GIC to rapid thermal treatment produces fast volatilization of the intercalant. Highly expanded graphite (EG) produces layered structures, with in-plane electrical conductivity similar to that of natural flake graphite but larger layer spacing[35–38] and higher volume expansion ratio (i.e., the ratio of the packing volume of EG to that of GIC).[36–38] Relatively little is understood of EG serving as conductive fillers in polymer–matrix composites. Recently, several investigators reported a markedly lower volume fraction of EG to reach a percolation threshold in different engineering polymeric systems.[39–43] The reported EG filler thickness varied from 10 to 50 nm based on TEM results. In such nanocomposites, the monomers were first introduced into the pores of the expanded graphite, followed by polymerization. In this article, we report the preparation of EG-reinforced HDPE by melt processing using a compounder. The effect of EG on melt viscosity was studied. The data are useful for examining the potential of mass producing expanded graphite for composite fabrication.

EXPERIMENTAL

Preparation of EG-reinforced HDPE

The expanded graphite (EG) was prepared according to the procedure described in our previous reports.[29,30] HDPE with brand of Philips Marlex 5502 was supplied by Philips Singapore Co. All HDPE pellets, graphite, and expanded graphite were dried at 60°C in a vacuum oven for 24 h. EG-reinforced HDPEs were prepared by melt processing. A Haake mixer (Haake, Bersdorff, Germany) and twin-screw extruder were used to compound the samples. Filler content is given in weight percentage (wt %) unless otherwise specified. HDPE/UG5 indicates 5 wt % of untreated graphite (UG), whereas HDPE/EG3 indicates 3 wt % EG in HDPE.

Melt mixing in a Haake mixer

Untreated graphite (UG) and expanded graphite (EG) fillers were mixed with HDPE, respectively, in a mixer (Haake Rheocord) at 200°C. The components were mixed for 20 min at a rotation speed of 20 rpm. The equilibrium torque was recorded automatically by the machine. The mixed material was compression molded into thin sheets with a thickness of 0.5 mm in a hot press at 200°C before testing.

TABLE I
Processing Conditions in the Twin-Screw Extruder for the Preparation of the EG- and UG-Reinforced HDPE

Zone (°C)					
1	2	3	4	Die (°C)	Screw speed
185	190	200	200	175	50 rpm

Twin-screw extrusion and injection molding

Melt blending was additionally carried out using a corotating twin-screw extruder (Leistritz Micro 18; with a screw diameter of 18 mm and an L/D ratio = 30). Table I shows the processing conditions in the twin-screw extruder for the preparation of the composites. The extruded pellets were injection molded into 3.5-mm-thick dogbone-shape specimens (ASTM D638 type I) using a Battenfeld BA 300 injection-molding machine. The temperatures in zone 1 and zone 2 were kept at 200 and 190°C, respectively. The nozzle temperature was kept at 175°C and the mold temperature was 30°C. An injection pressure of 70 bar and holding time of 50 s were used. The screw speed was kept at 140 rpm. All the materials were dried at 60°C for at least 24 h in a vacuum oven before processing.

Electrical conductivity test

The conductivity of UG- and EG-reinforced HDPE was measured using a dispersible four-point resistivity probe system (SIGNATONE) with a minimum limit of 10^{-8} S/cm. The hot pressed sample was cut into specimens of $10 \times 4 \times 0.5$ mm^3 for testing. For samples obtained from HDPE and its composites of lower filler content, the conductivity was below the detectable range of a four-point resistivity probe and thus a digital-mode resistivity determiner (RP2680) was used. Both instruments were sensitive to the limits prescribed by the manufacturers and the data so obtained were assumed to be comparable.

Thermal analysis

Thermal analysis was carried out on a modulated differential scanning calorimeter (DSC; Model MDSC 2920; TA Instruments, New Castle, DE). Before recording, the Haake-mixed or injection-molded specimen was heated quickly to 200°C and maintained for 10 min to erase the thermal history. The sample was cooled to room tem-

perature at a cooling rate of 10°C/min to obtain the cooling curve. The sample was then heated to 200°C at a heating rate of 10°C/min to study the melting behavior of HDPE. The entire thermal scan was conducted under inert N_2 with a gas flow rate of 50 mL/min.

Tensile test

The tensile tests to determine the tensile strength and modulus were performed according to the ASTM D638 using an Instron 5565 (Instron, Canton, MA) at a crosshead speed of 5 mm/min. The dimensions of the injection-molded tensile specimens were 60 × 10 × 3.5 mm^3. An extensometer was used to directly monitor the strain variation and to determine the modulus. The values reported were averages of five measurements.

Dynamic mechanical analysis

Dynamical mechanical analysis (DMA) experiments were conducted using a TA Instruments DMA 2980 in film tension mode at a fixed frequency of 1 Hz. The sample dimensions were 20 × 8 × 0.5 mm^3. The sample was tested with a temperature ranging from room temperature to 120°C at atmospheric pressure and a heating rate of 3°C/min.

RESULTS AND DISCUSSION

Effect of EG on melt viscosity

Torque rheometry measures the work accomplished in the studied materials during melt mixing under controlled conditions (i.e., temperature and shear rate). Torque is directly proportional to the melt viscosity at a certain time. Figure 1 illustrates the variation of equilibrium torque of the composites with different filler levels and filler types. The torque of unreinforced HDPE is 0.8 Nm. As the fillers were added into the HDPE, melt viscosity increased. However, the extent to which the fillers affected the viscosity of the HDPE matrix differed. As shown in Figure 1, for the same filler content introduction of EG increases the melt viscosity more dramatically than the case with UG. This difference suggests some interesting behavior of the EG in the HDPE matrix compared to that of the UG. As revealed in our previous studies, EG possesses a higher surface area-to-volume ratio and a higher form factor.[29,30] The increased surface area is likely to enhance the intercalation between EG and HDPE and subsequently melt deformation is hindered. The higher surface area of EG provided a better chance of the filler interactions with HDPE matrix during melt mixing.[44] It was previously shown that increased filler aspect ratio results in a higher viscosity of the mixtures in maleated PP–clay nanocomposites.[45] The higher surface area and filler aspect ratio of EG contribute to the more distinctive torque increase in EG containing HDPE compared to the UG-containing system.

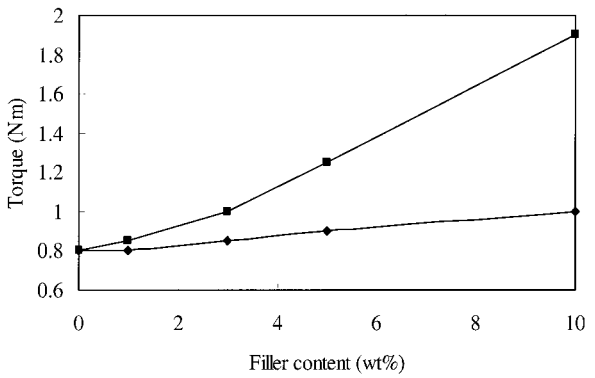

Figure 1 Torque of unreinforced and reinforced HDPE as a function of filler content in a Haake mixer at 200°C with a screw speed of 20 rpm. (■) EG; (◆) UG.

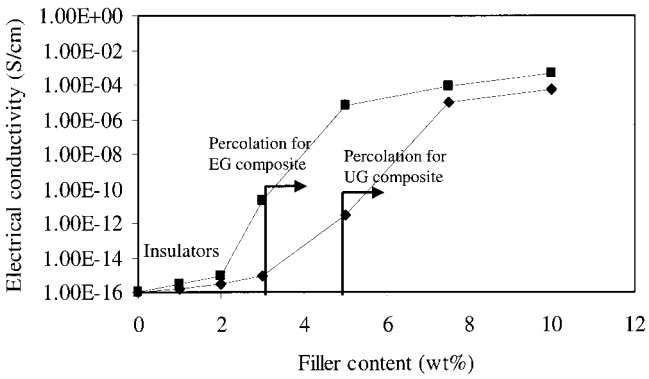

Figure 2 Electrical conductivity of the UG- and EG-reinforced HDPE as a function of filler content. (■) EG; (◆) UG.

Electrical conductivity of EG containing HDPE

Figure 2 compares the electrical conductivity of EG- and UG-containing HDPE. The conductivity of HDPE is about 10^{-16} S/cm,[46] which shows HDPE is an insulator. A rapid increase in electrical conductivity takes place when filler content exceeds 2 wt %. This increase appears, however, less dramatic in comparison with our previously reported PMMA reinforced with expanded graphite phases,[29,30] whereby only 1 wt % was required to reach the percolation threshold (ϕ_c). The percolation threshold corresponds to the onset of transition from an insulator to a conductor.[47] The increase in conductivity spans across 5 wt % of filler content (see Fig. 2) before the conductivity gradually levels off. At 3 and 5 wt % of reinforcement level, conductivity for the EG-filled system is 5 to 6 orders of magnitude higher than that of the untreated system (UG). In fact, the conductivity with 3 wt % EG is higher than that with 5 wt % UG. Clearly, the conductivity critically depends on how the graphite is ex-

TABLE II
Comparison of the Reported Percolation Threshold (ϕ_c) in EG and Carbon Black (CB) Filled Polymer Systems

Matrix	HDPE	PMMA[30]	PA6[40]	PS[43]	Epoxy[39]	PA6[25]	PP[25]	PMMA[27]
Filler	EG	EG	EG	EG	EG	CB	CB	CB
ϕ_c	3 wt %	1 wt %	1.5 wt %[a]	1 wt %	2.5 wt %[a]	9 wt %	6.2 wt %	8.0 wt %

[a] The filler weight fraction is calculated from the volume fraction provided in Refs. 39 and 40, assuming densities of 1.1, 1.2, and 2.2 g/cm^3 for PA6,[40] epoxy,[39] and EG,[32] respectively.

panded and dispersed in the HDPE matrix. The graphite fillers were examined using SEM in our previous studies.[29,30] Using an image-analysis software, the average sheet size for EG filler is quantified at about 20 μm and the average thickness 100 nm. The average graphite sheet size for UG is estimated at about 0.4 mm; the sheet thickness is estimated to be 5 μm. As a result the average form factors for EG and UG composites are 200 and 80, respectively. Clearly, the difference in conductive behavior can be attributed to the difference in filler form factor. Note that not all graphite phase is in completely expanded form. The difference in conductive behavior narrows as the filler content continues to increase. The results indicate there exists a saturation of filler at 7.5 wt % and further increase in graphite materials does not contribute to a more pronounced increase in conductivity. The transport mechanisms are viewed as similar to our previously reported case for graphite-filled PMMA, which complies with the percolation theory.[18,29]

Table II shows the comparison of the reported ϕ_c from PMMA, HDPE, CB, and other common fillers in polymeric matrices. The difference in ϕ_c (3 wt % for EG and 5 wt % for UG) is attributed to the filler form factor and the graphite network formation in the matrix. Generally, ϕ_c is higher in HDPE than that in PMMA. This suggests the conductive network formed by EG and UG in a HDPE matrix is less efficient than that in PMMA.[29,30] Three factors are likely to contribute to their difference.[1] Melt viscosity for mixing HDPE with fillers is higher than the viscosity of PMMA in solution blending.[30] Increased viscosity prevents the molecular chains to efficiently intercalate into the minipores of graphite fillers.[2] Blending through mechanical mixing in a Haake mixer induces filler damage and subsequently reduces the efficiency of network formation in the polymer.[3] Graphite fillers are more likely to form aggregates, which hinder dispersion, in mechanical blending. Nevertheless, the ϕ_c displayed for HDPE composites under melt compounding is still sufficiently low compared to that of other conventional carbon black (CB) fillers (see Table II) for mass production objectives.

Thermal analysis

HDPE is a semicrystalline polymer. The crystallinity of HDPE is closely related to its density. The crystallinity of HDPE (X_0) can be calculated based on the equation[46,48]

$$X_0 = \frac{d_c(d - d_a)}{d(d_c - d_a)} \quad (1)$$

where d is the density of the HDPE, d_c is the density of 100% HDPE crystal (0.985 g/cm^3), and d_a is the density of completely amorphous HDPE (0.824 g/cm^3). The density d of HDPE used for the matrix in this experiment was 0.958 g/cm^3, so the calculated crystallinity of HDPE was about 86%. The presence of graphite fillers is likely to influence the crystallization of HDPE. The latter will also affect the mechanical performance of the resulting composites. The crystallinity of HDPE (X) in the composites can be calculated based on the following equation:

$$X = X_0 \times \frac{\Delta H}{\Delta H_0} \quad (2)$$

where ΔH_0 is the crystallization enthalpy per gram of pure HDPE in the cooling run from DSC, and ΔH isthe crystallization enthalpy per gram of HDPE in composites.

Figure 3 displays the DSC cooling scans of the EG-containing HDPE together with HDPE alone after Haake mixing as a sample at a cooling rate of 10°C/min. Same trends were observed for the injection-molded specimens. The crystallization temperature (T_c) for both EG- and UG-containing HDPE is plotted as a function of filler content in Figure 4. The degree of crystallinity is plotted against filler content in Figure 5. Clearly, the crystallization temperature shifts toward the right as filler content increases (see Fig. 3). Again, the increase in T_c for the UG system is less dramatic than the EG system as shown in Figure 4. This outcome is rather consistent with other reinforcement types such as glass and carbon fibers.[49–51] The filler serves as a nucleating agent to induce crystallization at a higher temperature. With EG the filler tends to activate crystallization with a higher rate of increase in T_c versus filler content. This is understood because the EG possesses a higher surface-to-volume ratio than that of the UG in the HDPE matrix, causing more nucleating sites to be formed. In Figure 5, however, the relative crystallinity decreases as filler content in-

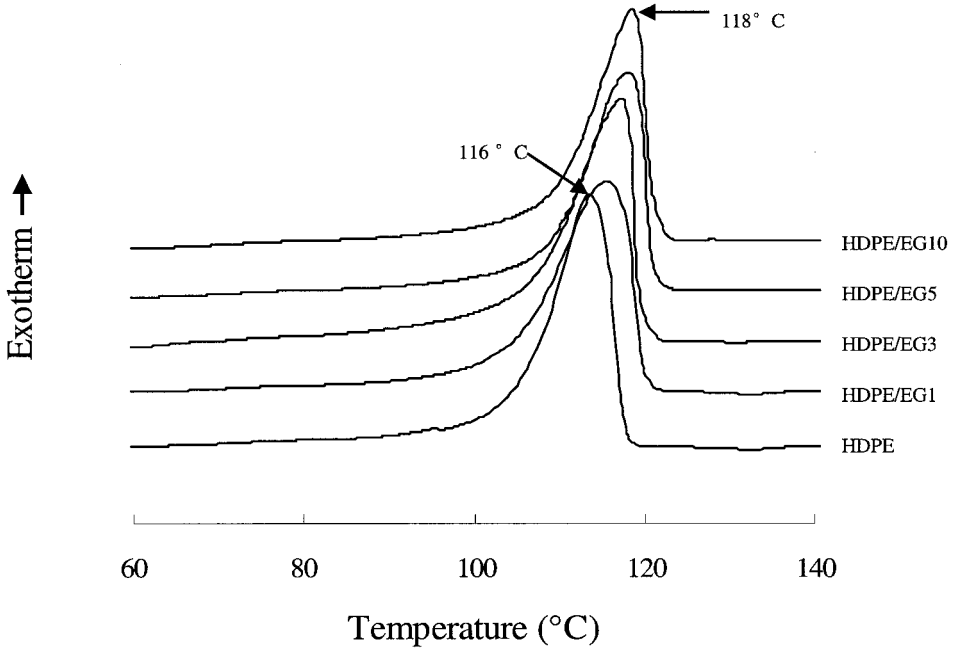

Figure 3 DSC cooling curves of HDPE and EG-containing HDPE. The last digit to the right indicates the filler wt % for each composition. The cooling rate is 10°C/min.

creases. It is conjectured without detailed microscopic evidence that the crystalline domains formed by HDPE are rendered smaller in the presence of graphite particles and reduce the overall crystallinity as the filler content increases. It is possible for the fillers to decrease the mobility of HDPE chains in the formation of crystallites and, as a result, the domains of crystalline phase are reduced in size.

It is also likely that imperfection of crystals in the presence of inhomogeneities contributes to the decrease in crystallinity. Apparently, the EG system is expected to show higher crystallinity compared to that of the UG system because for the former better dispersed inhomogeneities are present in inducing crystallization. Figure 6 shows the melting endotherms of HDPE in composites. At 10 wt % filler content, the melting temperature for EG containing HDPE (132°C) is the lowest, followed by UG (133°C) and unreinforced HDPE (134°C). Based on the Nishi and Wang theory,[52] the Flory–Huggins interaction parameter (χ_{12}) can be deduced from the melting temperature of HDPE in the composites. The decrease of melting temperature of HDPE in composites means some interactions between fillers and matrix. The stronger interaction was revealed in EG containing HDPE, which is in conformity with the rheometry results. A noteworthy point from Figures 2 and 4 is the sudden rise in crystallization temperature, which coincides

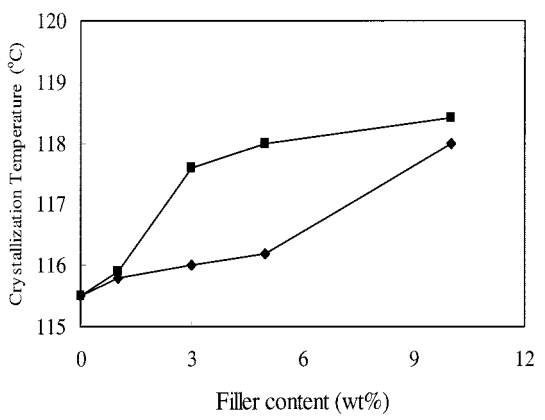

Figure 4 Crystallization temperature of HDPE and its composites versus filler content. (■) EG; (◆) UG.

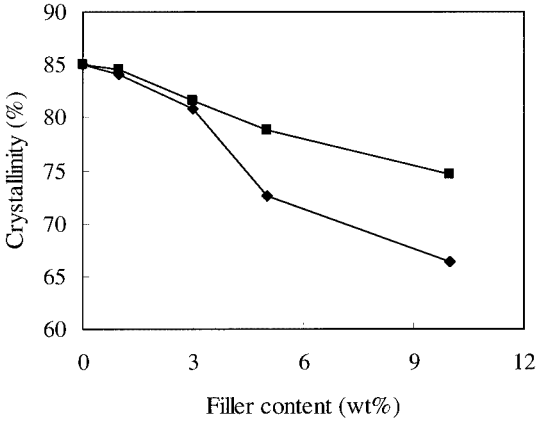

Figure 5 Crystallinity of reinforced HDPE versus filler content. (■) EG; (◆) UG.

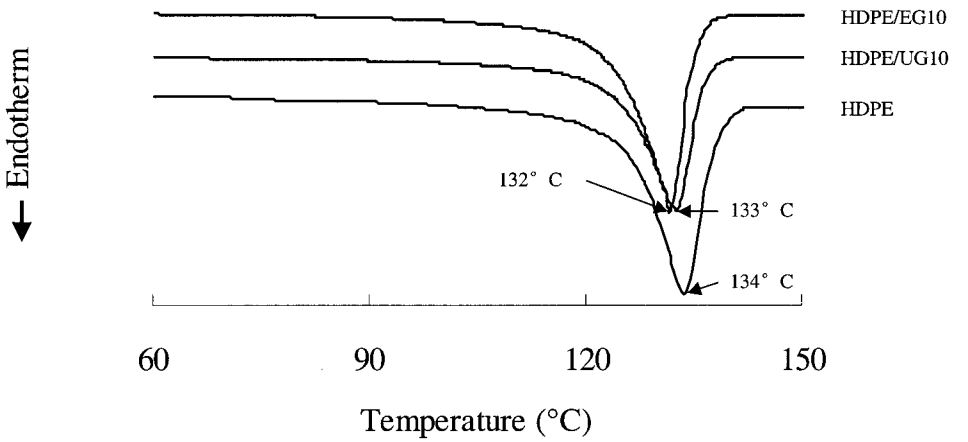

Figure 6 DSC heating curves of unreinforced HDPE, 10 wt % UG- and EG-reinforced HDPE. The heating rate is 10°C/min.

well with the percolation transition in electrical conductivity, for EG. This coincidence near 3 wt % strongly suggests the transport mechanisms are critically dependent on the conductive network formed by the EG with an improved surface-to-volume ratio.

Mechanical properties

Tensile test

To investigate the effect of EG on the mechanical properties of the composites, the injection-molded standard specimens were tested with a crosshead speed of 5 mm/min. Figure 7 shows some representative stress–strain curves of HDPE and 3 wt % UG- and EG-reinforced HDPE. Clearly the presence of fillers slashes the ductility of the unreinforced HDPE, which shows necking without break in a tensile test. Tensile failure depends critically on the localized deformation. Comparing the ductility of UG- and EG-containing HDPE, it appears the embrittlement effect is more severe in the UG system. The result indicates that the unexpanded graphite phase, characterized by relatively large inhomogeneities in the HDPE matrix, is more likely to introduce premature flaws, raising localized stress before fracture. This point, although intuitively understood, requires more microscopic evidence in our future work. Table III summarizes the averaged data of the tensile properties of the studied samples.

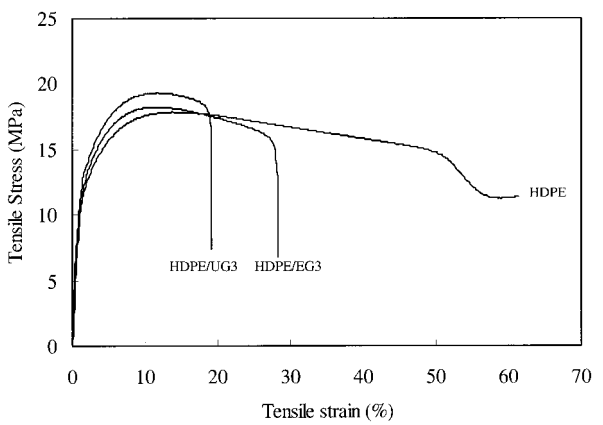

Figure 7 Tensile stress–strain curves of unreinforced HDPE, 3 wt % UG- and EG-reinforced HDPE. The crosshead speed is 5 mm/min.

The tensile modulus is measured from the initial region of tensile deformation and indicative of the composite value of the constituent stiffnesses. Both EG- and UG-containing HDPEs show higher tensile moduli than that in unreinforced HDPE. Comparing the EG to the UG systems, however, the former exhibits higher stiffness across the weight fractions up to 5 wt %. The improvement in tensile modulus is an expected outcome in view of the reinforcement effect from the graphite particles. Overall, the tensile modulus increased by 17% from 0% (1.25 MPa) to 3 wt % EG (1.46 MPa) and the reinforcement effects are not impressive. However, it can be reasonably established that stiffness improvement arises because of the higher stiffness values of the graphite components instead of increased crystallinity (see Fig. 5) in the given matrix. As verified in Figure 5, a further increase in filler content lowers the degree of crystallinity in the HDPE phase. As a result, the mechanical strength and stiffness of the matrix materials are projected to be lower compared to those of the unreinforced HDPE. Yet the incorporation of graphite fillers elevates the overall stiffness under uniaxial loading and displays a higher stiffness. Moreover, the EG fillers appear to demonstrate higher stiffness values compared to the UG ones at a given filler volume fraction according to the composite theory. The unimpressive stiffness improvement is attributed to the poor filler–matrix interface, which prohibits an effective load transfer from the matrix to the filler.

TABLE III
Tensile Results of Unreinforced and Reinforced HDPE with Filler Content of 3 wt %

	Tensile modulus (MPa)	Tensile strength (MPa)	Elongation at break (%)
HDPE	1.25 ± 0.02	18.0	>70[a]
HDPE/UG3	1.38 ± 0.03	19.3 ± 0.6	19.1 ± 1.0
HDPE/EG3	1.46 ± 0.02	18.7 ± 0.4	28.0 ± 0.7

[a] Specimens did not break.

Dynamic mechanical properties

Figure 8 shows a sample of the storage modulus E' for EG-containing HDPE as a function of temperature. Figure 9 plots E' at room temperature as a function of filler content. E' increases with filler content for both EG and UG systems. However, the increase in EG composites is more significant than that in the UG system. Almost a twofold increase in E' is noted with 10 wt % EG. At 5 wt % the increase in E' is estimated to be 50% and is more significant than the 17% increase with the engineering tensile tests. The more significant improvement in E' over that in E is attributed to the size and strain rate effects because the specimens tested under the film-tension mode in the DMA are comparatively smaller than the tensile specimens and the test rate used for the tests are different. E' was measured under cyclic loading with a strain rate of 1 Hz and E was measured at a quasi-static rate of 5 mm/min. Furthermore, the processing histories of the compression- and injection-molded specimens were also slightly different. The E' was obtained from a Haake mixed sample compression molded into 0.5-mm-thick sheets, whereas E was measured from extruded and injection-molded dogbone-shape samples. The former was less likely to exhibit thermal degradation in the compounding process. Nevertheless, the measurements show quite consistent trends, that is, the reinforcement effect for the EG system is more dramatic than that for the UG system. This is attributed to the expanded graphite phase whereby interfacial surface area-to-volume ratio increases and the filler form factor is improved in the HDPE matrix.

CONCLUSIONS

In this study, we focused on comparing the electrical and mechanical properties of two different graphite-reinforced HDPEs: one with UG and one with EG. The materials were mechanically mixed in extruders. Apparently, the EG system demonstrated better properties arising from a higher surface area and, as a result, a higher aspect ratio, compared to the UG system. Some specific conclusions could be drawn as follows:

1. The materials studied were fabricated in a melt-compounding process and demonstrated useful properties for antistatic coating, substrate, barrier, and both mechanical and electrical applications. Future development of graphite- or graphene-based nanocomposites awaits better dispersion of the nanofillers in the polymer matrix and the control of percolation transition in applications.
2. Viscosity increased with the addition of graphite fillers. The introduction of EG increased the torque dramatically, whereas the increase for the UG-reinforced system was less. The difference was attributed to EG's higher area-to-vol-

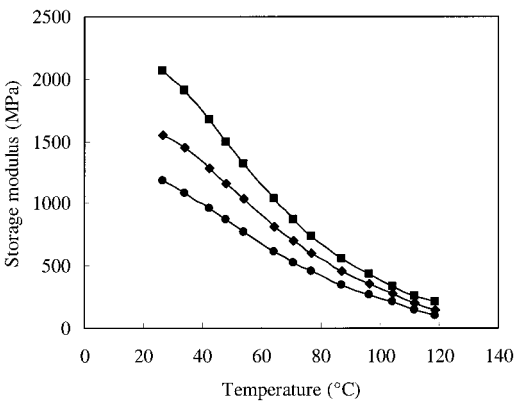

Figure 8 Storage modulus of graphite-reinforced HDPE of selected filler content versus temperature at 1 Hz frequency. (■) 3 wt % EG; (◆) 3 wt % UG; (●) unreinforced HDPE.

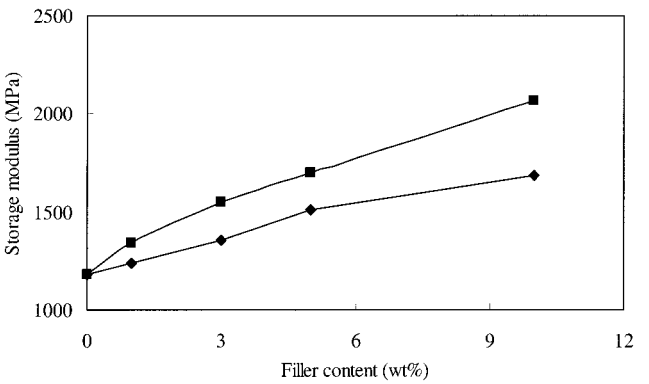

Figure 9 Storage modulus of UG- and EG-reinforced HDPE versus filler content. Temperature = 25°C. (■) EG; (◆) UG.

ume and aspect ratios, which promoted a more viscous flow in the HDPE matrix.

3. Electrical conductivity for the composites showed a transition from an insulator to a conductor. Only 3 wt % filler content was required to reach the percolation threshold (ϕ_c) for EG-containing HDPE, whereas significantly higher (5 wt %) filler content was required for the UG system. Overall, the transitions were not as sharp as in our previously reported PMMA system. An understanding of the transition would allow future design for nanocomposites using EG fillers.
4. The results from DSC of reinforced HDPE indicated that the fillers acted as nucleating agents to induce crystallization of HDPE in the composites. However, the degree of crystallinity of HDPE in composites decreased with an increase in the filler content, indicating the sizes of crystallites and crystalline phase decreased in the presence of inhomogeneities. Imperfection of crystals was also a likely contributor to the decreased crystallinity as the filler contented increased.
5. Both tensile and DMA measurements indicated EG was a better filler in the HDPE. Although the overall improvement in mechanical properties was not impressive, our results clearly confirmed the advantages of treating graphite in enhancing both the electrical conductivity and mechanical strength and stiffness of HDPE. The role of EG as a reinforcement phase was unambiguously established.

The authors thank Nanyang Technological University for funding this work and a nanomaterials grant (RGM–47/00) funding a research fellowship for W.Z. S.-C.W. acknowledges the financial support from ND NASA EPSCoR through NASA Grant NCC5-582.

References

1. Kojima, Y.; Usuki, A.; Kawasumi, M.; Okada, A.; Kurauchi, T.; Kamigaito, O. J Polym Sci Part A: Polym Chem 1993, 31, 983.
2. Vaia, R. A.; Teukolsky, R. K.; Giannelis, E. P. Chem Mater 1994, 6, 1017.
3. Giannelis, E. P.; Krishnamoorti, R.; Manias, E. Adv Polym Sci 1999, 118, 108.
4. Iijima, S. Nature 1991, 354, 56.
5. Fan, S.; Chapline, M. G.; Franklin, N. R.; Tombler, T. W.; Cassell, A. M.; Dai, H. Science 1999, 283, 512.
6. Zhang, X. X.; Li, Z. Q.; Wen, G. H.; Fung, K. K.; Chen, J.; Li, Y. Chem Phys Lett 2001, 333, 509.
7. Chen, L.; Wong, S. C. J Appl Polym Sci 2003, 88, 3298.
8. Kawasumi, M.; Hasegawa, N.; Kato, M.; Usuki, A.; Okada, A. Macromolecules 1997, 30, 6333.
9. Hasegawa, N.; Kawasumi, M.; Kato, M.; Usuki, A.; Okada, A. J Appl Polym Sci 1998, 67, 87.
10. Messersmith, P. B.; Giannelis, E. P. Chem Mater 1994, 6, 1719.
11. Lan, T.; Pinnavaia, T. J. Chem Mater 1994, 6, 2216.
12. Lan, T.; Kaviratna, P. D.; Pinnavaia, T. J. Chem Mater 1994, 6, 573–5.
13. Yano, K.; Usuki, A.; Okada, A. J Polym Sci Part A: Polym Chem 1997, 35, 2289–94.
14. Messersmith, P. B.; Giannelis, E. P. J Polym Sci Part A: Polym Chem 1995, 33, 1047–57.
15. Thostenson, E. T.; Ren, Z. F.; Chou, T. W. Compos Sci Technol 2001, 61, 1899.
16. Qian, D.; Dickey, E. C.; Andrews, R.; Rantell, T. Appl Phys Lett 2000, 76, 2868.
17. Gong, X.; Liu, J.; Baskaran, S.; Voise, R. D.; Young, J. S. Chem Mater 2000, 12, 1049.
18. Sichel, E. K. Carbon Black–Polymer Composites; Marcel Dekker: New York, 1982.
19. Ishigure, Y.; Iijima, S.; Ito, H.; Ota, T.; Unuma, H.; Takahashi, M.; Hikichi, Y.; Suzuki, H. J Mater Sci 1999, 34, 2979.
20. Pinto, G.; Jimenez-Martin, A. Polym Compos 2001, 22, 65.
21. Roldughin, V. I.; Vysotskii, V. V. Prog Org Coat 2000, 39, 81.
22. Flandin, L.; Bidan, G.; Brechet, Y.; Cavaille, J. Y. Polym Compos 2000, 21, 165.
23. Ray, S. S.; Biswas, M. Synth Met 2000, 108, 231.
24. Quivy, A.; Deltour, R.; Jansen, A. G. M.; Wyder, P. Phys Rev B 1989, 39, 1025.
25. Zois, H.; Apekis, L.; Omastova, M. In: Proceedings of the International Symposium on Electrets, 10th International Symposium on Electrets (ISE 10) 1999; pp. 529–532.
26. Mamunya, E. P.; Davidenko, V. V.; Lebedev, E. V. Compos Int 1997, 4, 169.
27. Gabriel, P.; Cipriano, L. G.; Ana, J. M. Polym Compos 1999, 20, 804.
28. Mallette, J. G.; Marquez, A.; Manero, O.; Castro-Rodriguez, R. Polym Eng Sci 2000, 40, 2272.
29. Zheng, W. G.; Wong, S. C.; Sue, H. J. Polymer 2002, 43, 6767.
30. Zheng, W. G.; Wong, S. C. Compos Sci Technol 2003, 63, 225.
31. Yudasaka, M.; Zhang, M.; Jabs, C.; Iijima, S. Appl Phys A 2000, 71, 449.
32. Dresselhaus, M. S.; Kalish, R. Ion Implantation in Diamond, Graphite and Related Materials; Springer-Verlag: Berlin, 1992.
33. Chung, D. D. L. J Mater Sci 1987, 22, 4190.
34. Cao, N. Z.; Shen, W. C.; Wen, S. Z.; Liu, Y. J.; Wang, Z. D.; Inagaki, M. Mater Sci Eng 1996, 14, 22 (in Chinese).
35. Toyoda, M.; Inagaki, M. Carbon 2000, 38, 199.
36. Liu, J. P.; Song, K. M. J Funct Mater 1998, 29, 659.
37. Furdin, G.; Marceche, J. F.; Herold, A. Fr. Add FR2682370, 1993.
38. Celzard, A.; Mareche, J. F.; Furdin, G.; Puricelli, S. J Phys D Appl Phys 2000, 33, 3094.
39. Celzard, A.; McRae, E.; Mareche, J. F.; Furdin, G.; Dufort, M.; Deleuze, C. J Phys Chem Solids 1996, 57, 715.
40. Pan, Y. X.; Yu, Z. Z.; Ou, Y. C.; Hu, G. H. J Polym Sci Part B: Polym Phys 2000, 38, 1626.
41. Xiao, P.; Sun, L.; Xiao, M.; Gong, K. In: Proceedings of the Materials Research Society Symposium, Boston, MA, 2001; p. 661, KK531-6.
42. Chen, G. H.; Weng, W. G.; Yan, W. L. J Appl Polym Sci 2001, 82, 2506.
43. Chen, G. H.; Wu, C. L.; Weng, W. G.; Wu, D. J.; Yan, W. L. Polymer 2003, 44, 1781.
44. Luo, S. J.; Wong, C. P. IEEE T Compon Pack T 2000, 23, 151.
45. Wang, K. H.; Xu, M. Z.; Choi, Y. S.; Chung, I. J. Polym Bull 2001, 46, 499.
46. Peacock, A. J. Handbook of Polyethylene Structures, Properties and Applications; Marcel Dekker: New York, 2000.
47. Xia, J.; Pan, Y.; Shen, L.; Yi, X. S. J Mater Sci 2000, 35, 6145.
48. Agranoff, J. Modern Plastics Encyclopedia; McGraw-Hill: New York, 1986.
49. Pisharath, S.; Wong, S. C. J Polym Sci Part B: Polym Phys 2003, 41, 549.
50. Mironov, V. S.; Park, M.; Choe, C.; Kim, J. K.; Lim, S. H.; Ko, H. H. J Appl Polym Sci 2002, 84, 2040.
51. Zhang, C.; Yi, X. S.; Asai, S.; Sumita, M. J Mater Sci 2000, 35, 673.
52. Olabisi, O.; Robeson, L. M.; Shaw, M. T. Polymer–Polymer Miscibility; Academic Press: New York, 1979.